Yi et al. Micro and Nano Syst Lett (2018) 6:17
https://doi.org/10.1186/s40486-018-0079-9

Micro and Nano Systems Letters

LETTER Open Access

Modulation of nanoparticle separation by initial contact angle in coffee ring effect

Johan Yi[1], Hwapyeong Jeong[1] and Jaesung Park[1,2,3*]

Abstract

The coffee ring effect occurs when a droplet of a suspension evaporates on a substrate; this process can separate suspended nanoparticles (NPs) by size as a result of geometric constraints at the contact line of the evaporating droplet. In the study, we used a polydimethylsiloxane (PDMS) stamp to make an even contact line, and we changed the contact angle θ of the droplet by selectively configuring hydrophilic and hydrophobic surfaces. In experiments, the temperature, relative humidity were held constant and glass was used as substrate. When the initial θ of the droplet was changed by using the PDMS stamp to coat the glass, NP separation was governed by θ, not by droplet volume V_D. When droplets had different initial θ but the same V_D, the NP separation in the droplet was ~8 μm at $\theta = 50°$, ~10 μm at $\theta = 30°$, and ~16 μm at $\theta = 14°$. This ability to increase the separation between particles by changing the initial θ of the evaporating droplet may allow clear separation of NPs in evaporating droplets.

Keywords: Particle separation, Initial contact angle, Droplet, Polydimethylsiloxane (PDMS) stamp

Introduction

When a droplet of a suspension dries on a substrate, a deposit of concentrated particles appears as a ring-shaped stain; this phenomenon is commonly known as the 'coffee ring' effect. The coffee ring effect was initially studied by Deegan et al. [1–3]. The effect was further studied for various purposes such as formation of the coffee ring [4], microarrays of DNA/RNA [5–7], ink-jet printing [8], crystallization [9], assembly of nanoparticles (NPs) [10–13], and biophysical detection [14, 15]. The coffee ring effect can separate particles by size; this ability has been exploited to simplify separation of NPs. However, the separation of NPs in the evaporating droplet should be improved to effectively distinguish unknown NPs by size. Some factors can be exploited to improve the particle separation. The Marangoni flow induced by a surface gradient can vary the position of the different sizes of NPs [16]. In this study, we focus on the geometry of the droplet because the mechanism of deposition of NPs is governed by a geometrical constraint that is imposed by the shape of the droplet [17].

The shape of the droplet can affect results of experiments related to the coffee ring effect. A droplet has a contact angle θ that depends on the surface energy of the liquid and the hydrophobicity of the substrate. θ affects the pattern of deposition, and therefore should be carefully controlled in experiments. The contact line (CL) of the droplet with the surface is also nonhomogeneous and uneven, so evaporation occurs asymmetrically. Particle separation occurs at the CL, and if it is not straight, the positions of the deposition of the particles vary, so the patterns of the coffee rings are inhomogeneous.

In this study, a polydimethylsiloxane (PDMS) stamp was used to construct hydrophilic and hydrophobic surface patterns on a substrate [18] to achieve a droplet that has a uniform CL, and to control initial θ by controlling the initial volume of the droplet. This approach enabled control of the modification of separations of different sizes of NPs that were suspended in the evaporating droplet. Use of the PDMS stamp achieved a uniform CL of the droplet, and the separation between NPs depended on θ.

*Correspondence: jpark@postech.ac.kr
[1] Mechanical Engineering, POSTECH, Pohang, Republic of Korea
Full list of author information is available at the end of the article

Materials and methods

Fluorescent polystyrene sphere beads (Magsphere and Thermo-Scientific) of 100 nm (red), 500 nm (green), 1 μm (blue) were diluted in deionized water of 15 ml. Ratio of particle number was 10: 4: 1 and number of 1 μm bead was 6×10^6. The particles have density of 1.05 g/cm^3. Slide glasses (76 mm × 52 mm × 1.2 mm) were used as substrates.

Photolithography was conducted on a 4-inch Si wafer. The wafer was first dehydrated for 10 min at 150 °C. SU-8 2050 photoresist (Microchem) was spin coated at 500 rpm for 20 s with 8 s of acceleration time, then spin coated at 4000 rpm for 50 s with 15 s acceleration time. Wafer was soft-baked at 90 °C for 6 min then exposed to a UV light (wave length = 380 nm, 10 mJ/s) for 20 s. Then the wafer was post-baked at 90 °C for 6 min, then developed using SU-8 developer (MicroChem) for 3 min. The wafer was then hard-baked at 120 °C for 20 min.

Polydimethylsiloxane (PDMS) resin (Dowhitech) and curing agent (Dowhitech) were mixed in 9:1 volume ratio. The mixture was poured onto the patterned wafer, then cured in an oven at 60 °C for 4 h, and cut to pieces 70 mm × 50 mm. The resulting patterns were used to impose hydrophobicity and hydrophilicity to glass substrates.

The droplet was evaporated in a thermally-controlled chamber (Fig. 1a). The temperatures of the cool surface (33 °C) and warm surface (35 °C) were controlled individually by independent water baths. The temperature difference induced a surface-tension gradient at depth of 1 mm. Air with constant temperature and relative humidity was maintained by the temperature and humidity chamber.

The experiment was conducted in five steps. (1) The glass was treated using oxygen plasma at 70 W for 2 min (Femto Science). (2) The PDMS stamp was immediately pressed on the glass for 1 min to transfer a hydrophobic pattern, then peeled off. (3) A droplet of solution with NPs was dropped on the hydrophilic pattern on the substrate (Fig. 2a). (4) The droplet was evaporated in the chamber under controlled temperature and humidity. (5) The residual ring was observed using a fluorescence microscope.

Result and discussion

The governing equation of the evaporating droplet is a vapor mass transfer equation: $\frac{dc}{dt} = D\nabla^2 c$, where c [mol/m^3] is the local liquid vapor concentration, t [s] is time, and D [m^2/s] is the vapor diffusivity. This equation can be simplified by neglecting the transient term by assuming quasi-steady state because of the slow evaporation of the liquid ($dc/dt = 0$) The droplet can be assumed to be a spherical cap, and the gravity effect can be neglected in a small droplet. The analysis considers Bond number $0.044 \leq Bo = \frac{\rho g R h}{\sigma} \leq 0.073$, which is the ratio of surface tension to gravitational force, and Capillary number $Ca = \frac{\mu V}{\sigma} \approx 10^{-7}$, which is the ratio of viscous force to surface tension, where ρ [kg/m^3] is the density of the liquid, $g = 9.8$ m/s^2 is the force of gravity at the Earth's surface, h [m] is the height of the droplet, R [m] is the radius of the droplet, μ [N s/m^2] is the liquid viscosity, and σ [N/m] is the surface tension of the liquid.

The process of using the PDMS stamp to coat the glass yielded a selective pattern of hydrophobicity and hydrophilicity that induced formation of a pattern of droplets on the glass (Fig. 2b). Three circular shapes of different diameters d [mm] were used for the experiment. Patterns coated by PDMS stamp remained for 30 h (Fig. 2c). Droplets with volume $V_D = 0.8$ μL were dropped on pattern 1 ($d = 1.98$ mm), pattern 2 ($d = 2.55$ mm), pattern 3 ($d = 3.18$ mm). The droplet above pattern 1 had $\theta_1 = 50°$ and the droplet above pattern 2 had $\theta_2 = 30°$. These θ did not change for 30 h after the PDMS stamping. However, the droplet above pattern 3 had $\theta_3 = 14°$ and this droplet changed its shape on the glass and could not fill the whole pattern; these results indicate that the hydrophobicity of PDMS film was retained for at least 30 h, and that hydrophilicity imparted by the air plasma was weakened. To obtain a small $\theta_3 = 14°$ effectively, the experiment should

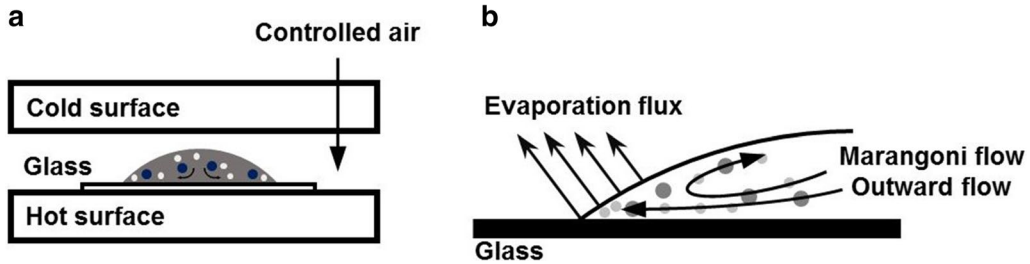

Fig. 1 **a** Experimental set of evaporation of droplet in temperature- and humidity-controlled chamber. **b** Flow of different-size particles at contact line of evaporating droplet

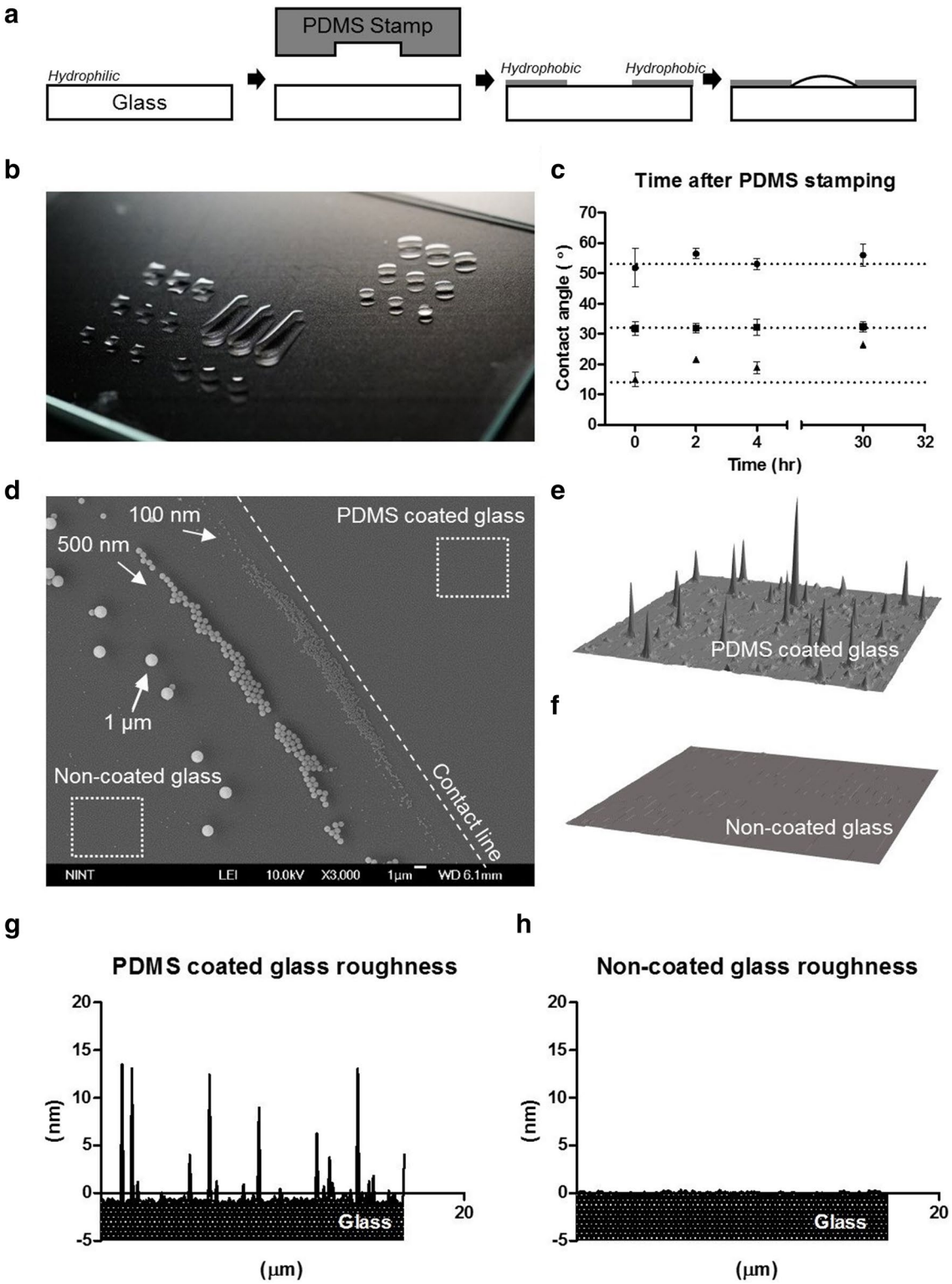

Fig. 2 **a** Schematic of PDMS-coated glass by PDMS stamp. **b** Image of patterned droplet on PDMS coated glass. **c** Contact angle of droplet vs. time after PDMS stamping. **d** SEM image of contact line of evaporated droplet with 100 nm, 500 nm, and 1 µm beads on PDMS-coated glass. AFM image of **e** PDMS coated area on glass and **f** non-coated glass. Surface roughness of **g** PDMS coated glass and **h** untreated glass

be performed immediately after PDMS stamping of the substrate.

The coffee-ring effect separated the 100 nm, 500 nm, and 1 μm NPs (Fig. 2d). The hydrophobic surface outside the pattern was partially coated by PDMS (Fig. 2e, f) with heights of ~10 to 15 nm (Fig. 2g), whereas the non-stamped area was smooth (Fig. 2h).

The coffee ring effect appears on a substrate where droplet has dried. The CL of the droplet is pinned due to the surface property of the substrate. Evaporation rate is highest at the rim of the droplet (Fig. 1b). The evaporation flux $\left(\vec{J}\cdot\vec{n}\right)$ was calculated by FEM analysis as described previously [2, 19, 20]: $\left(\vec{J}\cdot\vec{n}\right)=J_0\left(1-\tilde{r}^2\right)^{-\lambda(\theta)}$ where J_0 is the evaporation flux of the center of the droplet, $\tilde{r}$ is the ratio of radial distance r [m] to the radius R [m] of the droplet; $\lambda(\theta)$ is a fitting parameter that represents the non-uniformity of the evaporation flux of the droplet at different contact angles. The molecules at the outer edge of the droplet have higher probability of escaping than do molecules at the center of the droplet; i.e., loss of molecules increases with distance from the center the droplet. The mass loss rate of the droplet can be integrated from the evaporation flux: $-\dot{m}(t)=\pi RD(1-H)c_v\left(0.27\theta^2+1.30\right)$. The mass loss rate is proportional to R, diffusivity D [m^2/s], difference of vapor concentration $(1-H)c_v$ and increases quadratically as θ increases. The evaporation flux differs along the interface of the droplet.

This difference of evaporation flux drives an outward flow from the center to the rim of the droplet to compensate for liquid loss. The suspended NPs in the droplet are carried by the outward flow and deposited at the CL between the droplet and the substrate. After complete evaporation of the droplet, rings of concentrated NPs appear on the substrate.

Particle separation occurs when the suspended NPs in the droplet are trapped in the gap between droplet and substrate [17]. As a consequence, evaporation of the liquid causes the NPs to be aligned by size near the CL (Fig. 3); in theory, the position at which an NP is deposited depends on its size as $\Delta l=\Delta r$ tan (θ/2), where r is particle radius $\Delta r=r_2-r_1$, and Δl is separation distance. However, in a real system, measured Δl is longer than the calculated value.

The coffee ring effect can be weakened by the Marangoni effect [21, 22], which is caused by a surface tension gradient that is induced by a temperature gradient. The particles are concentrated at the center of the droplet by inward Marangoni flow. For effective separation, the Marangoni effect can be adjusted to the coffee ring effect in the evaporating droplet [23]. The Marangoni flow recirculates the particle along the interface of the droplet.

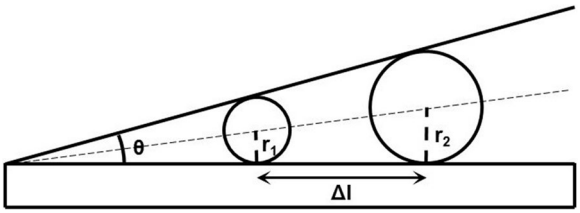

Fig. 3 Geometric constraints on approach to CL by NPs of different sizes. The NPs are sorted by size

Small NPs approach the CL more closely than large NPs do. The combination of the Marangoni flow due to temperature gradient and radial outward flow that is generated by difference in the latent heat of evaporation along CL allows simple separation of NPs that have sizes from nanometers to micrometers.

The PDMS stamp was used to make droplets that had the same initial θ but different V_D (Fig. 4a–c). The temperature of the chamber was ~34 °C, and relative humidity was ~50% with temperature gradient of 2 °C/mm in every experiment. The conditions of the air and the substrate were maintained constant to isolate the effect of the initial θ.

Different sizes of pattern ($d_1=1.98$ mm, $d_2=2.55$ mm, $d_3=3.18$ mm, $d_4=3.82$ mm) on a PDMS stamp were used to make the same θ. θ was controlled by adjusting V_D. The combination of the hydrophobicity of the surroundings of PDMS film and the hydrophilicity induced using air plasma, caused droplet capture in a pattern on the glass. After the droplets had been evaporated in the temperature- and humidity-controlled chamber, the separation of the 100 nm, 500 nm and 1 μm beads was almost same when the droplet had the same θ (Fig. 4d). The largest V_D was more than six time the smallest V_D, but this difference did not affect the particle separation.

To evaluate the effects of the initial θ of the droplet, PDMS stamp was used to make different initial contact angles $\theta_1=50°$, $\theta_2=30°$, $\theta_3=14°$ (Fig. 5a) with the same V_D. The condition of the evaporation was same as the previous system of particle separation. After the droplet had evaporated, fluorescent polystyrene beads with sizes of 100 nm, 500 nm, 1 μm were separated by size near the CL of the droplet. The separation between beads increased as θ decreased, from ~8.6 μm at $\theta_1=50°$ (Fig. 5b) to ~10 μm at $\theta_2=30°$ (Fig. 5c) to ~16.6 μm at $\theta_3=14°$ (Fig. 5d). This result indicates that reducing the θ increases the particle separation at given conditions of temperature, relative humidity, temperature gradient, volume, and particle concentration (Fig. 5e).

Particle separation has several uses. Bioparticles separate in the droplet by size, so the method can be used to measure particle size [17]. This method may have use in diagnosis of diseases. To use the separation of NPs effectively, the resolution of separation should be

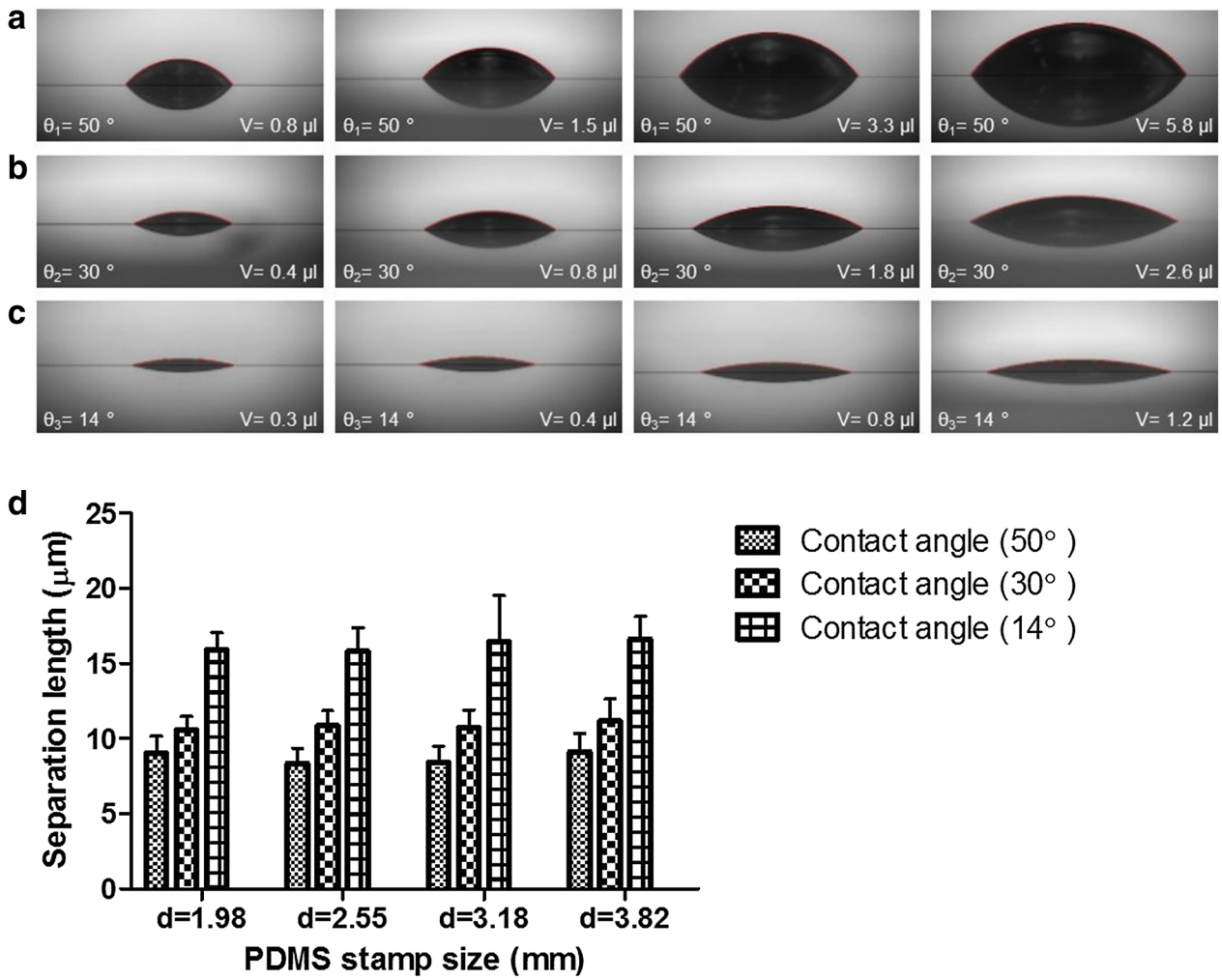

Fig. 4 Image of the droplet with same contact angle but different volumes **a** $\theta_1 = 50°$, **b** $\theta_2 = 30°$, **c** $\theta_3 = 14°$. **d** Separated length between 100 nm and 1 µm beads in the evaporated droplet with same contact angle but different volumes

improved. One method to achieve this goal may be to change the Marangoni flow by controlling the temperature gradient and change the type of substrate [16].

Here we focused on the fundamental mechanism by which NPs are deposited. We changed the initial contact angle of the evaporating droplet, and thereby allowed NPs of different sizes to align at different positions near the CL. Our results indicate that droplet that has small volume above pattern reduces the initial contact angle and allow the improved particle separation. This result matches to the principal mechanism of the deposition of the NPs in the evaporating droplet. This study will broaden the knowledge of particle separation.

Conclusion

The paper presents a simple method to separate NPs by size. A PDMS stamp was used to divide a surface into hydrophilic and hydrophobic areas. This division enabled formation of an even CL and allowed control of the contact θ angle of water droplets. θ and volume V_D of the droplet were changed, but the temperature gradient to produce the Marangoni flow, and relative humidity were maintained constant. The separation between NPs was controlled by the initial θ, but was not affected by V_D. The separation of the NPs in the evaporating droplet was affected by the initial contact angle because the NPs are aligned by their size at the CL due to the

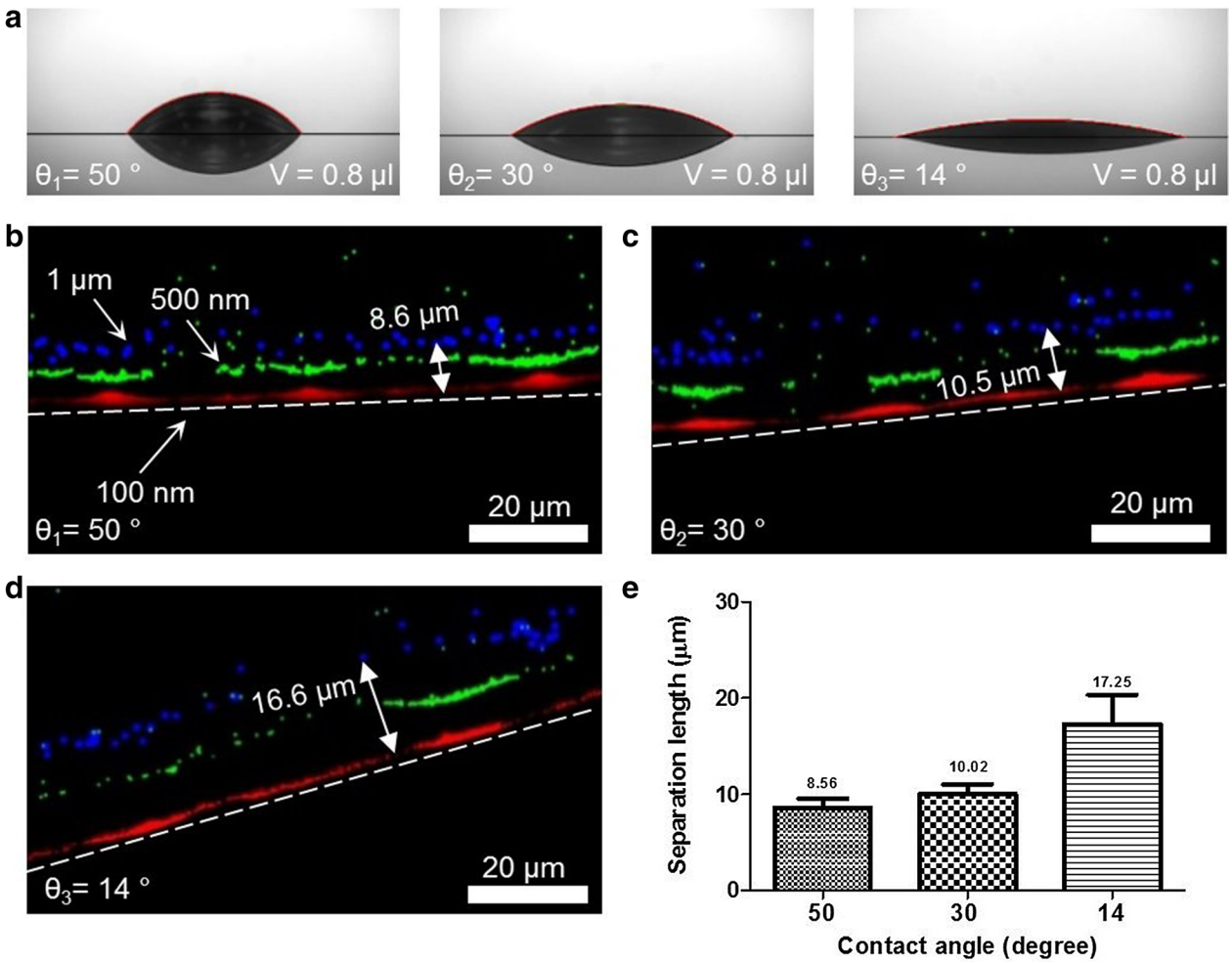

Fig. 5 Contact angle of droplet having same volume (0.8 µl) **a** $\theta_1 = 50°$, $\theta_2 = 30°$, $\theta_3 = 14°$. Fluorescence image of 100 nm, 500 nm, 1 µm beads in the evaporated droplet at **b** $\theta_1 = 50°$, **c** $\theta_2 = 30°$, **d** $\theta_3 = 14°$. **e** Separation between 100 nm and 1 µm beads varied with θ

geometric constraints in the droplet. Controlling the initial contact angle to ~ 14° will allow effective separation of NPs by size in an evaporating droplet when it undergoes the coffee ring effect.

Authors' contributions

JY, HJ, and JP designed the experimental strategy, analyzed data, and prepared the manuscript. JH performed particle-separation experiments and analysis, HJ designed the experimental system and analysis. All authors commented on the manuscript. All authors read and approved the final manuscript.

Author details

[1] Mechanical Engineering, POSTECH, Pohang, Republic of Korea. [2] School of Interdisciplinary Bioscience and Bioengineering, POSTECH, Pohang, Republic of Korea. [3] Center for Wireless Integrated MicroSensing and Systems, University of Michigan, Ann Arbor, MI 48109, USA.

Competing interests

The authors declare that they have no competing interests.

Availability of data and materials

The datasets supporting the conclusions of this article are included within the article.

Funding

This work was supported by the National Research Foundation of Korea Grant funded by the Korean Government (NRF-2018R1A2B3006280).

Publisher's Note

Received: 24 October 2018 Accepted: 19 December 2018
Published online: 24 December 2018

References

1. Deegan RD et al (1997) Capillary flow as the cause of ring stains from dried liquid drops. Nature 389:827

2. Deegan RD et al (2000) Contact line deposits in an evaporating drop. Phys Rev E Stat Phys Plasmas Fluids Relat Interdiscip Topics 62(1 Pt B):756–765
3. Deegan RD (2000) Pattern formation in drying drops. Phys Rev E Stat Phys Plasmas Fluids Relat Interdiscip Topics 61(1):475–485
4. Shen X, Ho CM, Wong TS (2010) Minimal size of coffee ring structure. J Phys Chem B 114(16):5269–5274
5. Pirrung MC (2002) How to make a DNA chip. Angew Chem Int Ed Engl 41(8):1276–1289
6. Jing J et al (1998) Automated high resolution optical mapping using arrayed, fluid-fixed DNA molecules. Proc Natl Acad Sci USA 95(14):8046–8051
7. Dugas V, Broutin J, Souteyrand E (2005) Droplet evaporation study applied to DNA chip manufacturing. Langmuir 21(20):9130–9136
8. Soltman D, Subramanian V (2008) Inkjet-printed line morphologies and temperature control of the coffee ring effect. Langmuir 24(5):2224–2231
9. Takhistov P, Chang H-C (2002) Complex stain morphologies. Ind Eng Chem Res 41(25):6256–6269
10. Choi S et al (2010) Coffee-ring effect-based three dimensional patterning of micro/nanoparticle assembly with a single droplet. Langmuir 26(14):11690–11698
11. Vakarelski IU et al (2009) Assembly of gold nanoparticles into microwire networks induced by drying liquid bridges. Phys Rev Lett 102(5):058303
12. Diao J, Cao Q (2011) Gold nanoparticle wire and integrated wire array for electronic detection of chemical and biological molecules. AIP Adv 1(1):012115
13. Diao J, Xia M (2009) A particle transport study of vertical evaporation-driven colloidal deposition by the coffee-ring theory. Colloids Surf A 338(1–3):167–170
14. Shao L et al (2014) Gold nanoparticle wires for sensing DNA and DNA/protein interactions. Nanoscale 6(8):4089–4095
15. Wen-Tao L, Jia-Jie D (2015) Colloidally deposited nanoparticle wires for biophysical detection. Chin Phys B 24(12):127308
16. Jeong H et al (2014) Nanoparticle separation using Marangoni flow in evaporating droplets. In: Solid-state sensors, actuators and microsystems workshop Hilton Head Island, South Carolina
17. Wong TS et al (2011) Nanochromatography driven by the coffee ring effect. Anal Chem 83(6):1871–1873
18. Li Y et al (2017) Rapid assembly of large scale transparent circuit arrays using PDMS nanofilm shaped coffee ring. Adv Func Mater 27(11):1606045
19. Hu H, Larson RG (2005) Analysis of the microfluid flow in an evaporating sessile droplet. Langmuir 21(9):3963–3971
20. Hu H, Larson RG (2002) Evaporation of a sessile droplet on a substrate. J Phys Chem B 106(6):1334–1344
21. Hu H, Larson RG (2005) Analysis of the effects of Marangoni stresses on the microflow in an evaporating sessile droplet. Langmuir 21(9):3972–3980
22. Hu H, Larson RG (2006) Marangoni effect reverses coffee-ring depositions. J Phys Chem B 110(14):7090–7094
23. Jeong H et al (2018) Analysis of extracellular vesicles using coffee ring. ACS Appl Mater Interfaces 10(27):22877–22882